This is the peer-reviewed, final accepted version for American Mineralogist, published by the Mineralogical Society of America.
The published version is subject to change. Cite as Authors (Year) Title. American Mineralogist, in press.
DOI: https://doi.org/10.2138/am-2021-7852. http://www.minsocam.org/

Revision 1

Word count: 7044 (Includes references, tables and figures with captions)

Ferromagnesian jeffbenite synthesized at 15 GPa and 1200ºC

Joseph R. Smyth[1], Fei Wang[2], Ercan E. Alp[3], Aaron S. Bell[1], Esther S. Posner[4], and Steven D. Jacobsen[2]

[1]*Department of Geological Sciences, University of Colorado, Boulder, CO 80309 USA*
[2]*Department of Earth and Planetary Sciences, Northwestern University, Evanston, IL 60208 USA*
[3]*Advanced Photon Source, Argonne National Laboratory, Argonne, IL 60439 USA*
[4]*Bayerisches Geoinstitut, Universität Bayreuth, Bayreuth, Germany*

ABSTRACT

Single crystals of Al-free, ferromagnesian jeffbenite up to 200 μm in size have been synthesized at 15 GPa and 1200 ºC in a 1200 tonne multi-anvil press from a starting composition in the forsterite-fayalite-magnetite-water system. This phase has the approximate formula $Mg_{2.62}Fe^{2+}_{0.87}Fe^{3+}_{1.63}Si_{2.88}O_{12}$ and is observed to co-exist with a Ca-free clinopyroxene plus what appears to be quenched melt. The crystal structure has been refined from single-crystal X-ray diffraction data and is similar to that determined for natural Al-bearing jeffbenite, $Mg_3Al_2Si_3O_{12}$, reported from inclusions in superdeep diamonds. The structure is a tetragonal orthosilicate in space group $I\bar{4}2d$ with a = 6.6449(4) Å; c = 18.4823(14) Å, and is structurally more closely related to zircon than to garnet. The T2 site is larger than T1, shares an edge with the M2 octahedron, and incorporates significant Fe^{3+}. Because of the tetrahedral incorporation of trivalent cations, jeffbenite appears to be compositionally distinct from garnet. Previous speculations that the phase may only occurs as a retrograde decompression product from bridgmanite are not supported by its direct synthesis under transition zone conditions. The phase has a calculated density of 3.93 g/cm^3, which is indistinguishable from a garnet of comparable

composition, and is a possible component in the mantle transition zone under oxidizing conditions or with Al-rich compositions.

Corresponding Author: Joseph R Smyth smyth@colorado.edu

Keywords: jeffbenite; TAPP (tetragonal almandine pyrope phase); super deep diamonds; diamond inclusions;

INTRODUCTION

Jeffbenite is a new mineral recently named and described as inclusions in diamonds thought to be of superdeep origin in the transition zone or lower mantle (Nestola et al, 2016). Previously termed TAPP, for tetragonal almandine-pyrope phase, the composition closely resembles that of Al-rich garnet. Armstrong and Walter (2012) reported the occurrence of this phase in laser-heated diamond anvil cell experiments at pressures of 6 to 10 GPa and 1300 to 1700 ºC, but it has not previously been synthesized in multi-anvil experiments. Recovery of large, synthetic single crystals will facilitate further study of the crystal chemistry and physical properties of jeffbenite.

The synthesis experiment was not designed to produce this phase. Woodland and Angel (1998) reported the crystal structure of a spinelloid III phase isostructural to wadsleyite existing on the fayalite-magnetite join at 6 GPa. This phase has the tetrahedral site half-occupied by ferric iron and the other half by Si. Exploratory multi-anvil experiments were conducted in the forsterite-fayalite-magnetite field under hydrous conditions to test for solid solutions between wadsleyite and spinelloid III. Bolfan-Casanova et al (2012) and Smyth et al (2014) noted that wadsleyite synthesized under oxidizing and hydrous conditions may incorporate up to 25% ferric iron in the tetrahedral site This raises the question of whether there might be complete solid solution between the wadsleyite field at 13-18 GPa and the ferric-iron-rich spinelloid III from Woodland and Angel (1998) on the fayalite-magnetite join at 6 GPa.

One such experiment in our exploration of the forsterite-fayalite-magnetite system at 15 GPa and 1200ºC produced an unrecognized Fe-rich silicate phase co-existing with what appeared to be a quenched liquid and Ca-free clinopyroxene. Single-crystal X-ray diffraction experiments were carried out to characterize the iron silicate phase. Examination of three crystals all show a

body-centered tetragonal unit cell with lattice parameters of about a = 6.6 Å and c = 18.4 Å, consistent with the recently-discovered jeffbenite phase, ideally $Mg_3Al_2Si_3O_{12}$ in space group $I\bar{4}2d$ (Nestola et al. 2016). Here, we report the synthesis of ferric-iron-rich, Al-free jeffbenite at transition zone P-T conditions, recovered to ambient for characterization and physical properties measurements. Along with the structure from X-ray diffraction, Raman, FTIR, and synchrotron-Mössbauer spectra are presented. This phase may be a stable phase in the mantle transition zone capable of accommodating significant amount of ferric iron through redox reactions in the deep mantle.

There have been several reports of the tetragonal almandine-pyrope phase (TAPP), now known as jeffbenite, as inclusions in diamonds thought to be of ultra-deep origin, particularly from the Juina region of Brazil (Harte et al., 1999; Harris et al., 1997; McCammon et al 1997; Walter et al., 2011; Bulanova et al., 2010; Hayman et al., 2005; Zedgenizov et al. 2020). Ideal compositions for this phase are reported to be identical to that of pyrope garnet. However, chemical analyses by these authors all show fewer than 3.0 Si, and fewer than three divalent cations, per 12 oxygens with Al being the major trivalent cation, but with significant amounts ferric iron and Cr. The crystal structure of this phase was reported by Harris et al. (1997) and re-examined by Finger and Conrad (2000). A refinement of the crystal structure parameters was also reported by Nestola et al. (2016). Because of the close overlap in composition of this phase with garnet, and its occurrence in diamonds thought to be of ultra-deep origin, Walter et al. (2011) and Armstrong and Walter (2012) suggested that the phase may be a metastable quench product from bridgmanite. Armstrong and Walter (2012) reported the occurrence of this phase in diamond-anvil experiments, but large crystals suitable for property measurements have not been synthesized in multi-anvil experiments.

SYNTHESIS

Synthesis was carried out in a 10/5 assembly (10mm octahedron with 5mm corner truncations on WC cubes) in the 1200 tonne Sumitomo multi-anvil press at Bavarian Institute for Experimental Geophysics and Geochemistry at University of Bayreuth, Germany. The starting composition consisted of mixed oxide powders of FeO, Fe_2O_3, SiO_2, MgO and $Mg(OH)_2$ with a total estimated water content of 3.0 weight percent H_2O The composition was placed in a welded 1.2 mm Pt capsule with 0.10 mm wall thickness. The assembly was ramped to pressure over four hours and then heated to 1200ºC for 4.5 h duration. Although H and Fe loss to the capsule was to be expected, the volume of the capsule wall is very small relative to the volume of the experiment charge, so losses are not expected to be significant. The capsule was mounted in epoxy and ground and polished to expose the capsule mineral assemblage. The capsule contained what appeared to be an extremely fine-grained quenched melt, a band of apparently single-phase, dark-colored to opaque crystals up to 200 μm in longest dimension, and a third phase identified by single crystal X-ray diffraction as a primitive ($P2_1/c$) clinopyroxene.

CHARACTERIZATION

Electron microprobe

Compositional analyses were acquired on a JEOL 8230 electron microprobe at the University of Colorado, Boulder. The EMP analyses were performed at a beam energy of 15 keV, a 20 nA beam current, a beam diameter of 1 micron, and a 40 degree takeoff angle. The on-peak and off-peak counting times were set to 30 seconds for all elements. Both unknown and standard intensities were corrected for detector dead time. The matrix correction applied to the raw data was the Pouchou and Pichoir-Full (PAP) algorithm and the mass absorption coefficients

were from the NIST FFAST database. The excess oxygen required to charge balance ferric iron was also included in the matrix correction. Results of the microprobe analyses are reported in Table 1. The ferrous-ferric ratio from Mössbauer was used here, and the slight excess of cations is likely due to a minor oxidation state gradient across the sample.

X-ray diffraction

Single-crystal X-ray diffraction was carried out on a Bruker P4 four-circle X-ray diffractometer with an APEX II detector system. The X-ray source was a Bruker 18 kW rotating Mo-anode generator operated at 50 kV and 250 mA with incident graphite monochromator. The crystals were 50 to 120 μm in size and mounted on a glass fiber. Five crystals were examined and all gave similar body-centered tetragonal unit cells with a = 6.64 Å and c = 18.5 Å. A data collection out to 75º 2θ was measured yielding 12871 intensities, of which 1061 were unique. Systematic absences were consistent with the acentric space group $I\bar{4}2d$.

Crystal structure refinement was carried out using SHELXL version 2016/4. Initial atom position parameters were those of Al-rich jeffbenite (Nestola et al., 2016). The refinement converged to R1 = 0.037 using anisotropic displacement parameters and ionized atom scattering factors for Mg^{2+}, Fe^{2+}, Si^{4+}, (Cromer and Mann, 1968) and O^{2-} (Azavant and Lichanot, 1993). The space group is acentric, so there are two possible absolute structures. The Flack x parameter for this model was 1.02(7), so the structure was inverted and the refinement repeated. The largest residual electron density of 2.1 $e^-/Å^3$ for this model was only 0.456 Å away from the T2 cation, consistent with two different cations occupying the site. Refinement of site occupancy at T2 indicated significant substitution for Si by iron, presumably ferric iron. The presence of residual electron density near this site indicated that the heavier cation might occupy a slightly

different position. The *x/a* position parameter for this site was allowed to vary for the Fe and Si positions and the R reduced further to 0.0278. Refinement and data parameters are given in Table 2; and selected cation-oxygen distances and coordination parameters in Table 3. Final positional and displacement parameters are available in the accompanying CIF file. Electrostatic site potentials were calculated using the program ELEN (Smyth, 1988) assuming nominal integer charges of +2 for M1 and M3, +3 for M2, +4 for T1 and T2, and -2 for the oxygen positions. These are also reported in Table 3. A polyhedral drawing of the crystal structure is given in Figure 1.

Raman spectroscopy

Raman spectra were obtained from 0-4500 cm^{-1} using a custom-built, confocal micro-Raman spectrometer with 458 nm excitation laser, Olympus-BX microscope, Andor Shamrock i303 spectrograph and Newton DU970 EMCCD camera. Because of the dark color of the Fe-rich jeffbenite, the laser power was reduced to ~5 mW at the focal point of about 1-2 um in size through a 100x objective. Spectra were obtained using a 1200 lines/mm diffraction grating and collected for 30 seconds, averaged over 6 accumulations. Raman spectra taken on the same crystal used for the X-ray diffraction data collection (sample B8) and a second crystal chosen at random are shown in Figure 2.

FTIR spectroscopy

To investigate the possibility of OH defects in ferromagnesian jeffbenite synthesized under hydrous conditions, unpolarized infrared absorption spectra were obtained at 500-4000 cm^{-1}. Because the material is very dark blue in color, even in thin section, it was necessary to polish crystals to <30 μm thickness. Polishing was done by mounting crystals onto a frosted glass slide with cyanoacrylate adhesive and thinned by gentle grinding with 3 μm diamond lapping film and

finished with an optical polish using 1 μm diamond film. The procedure was carried out on both sides to produce parallel plates of varying thickness. The cyanoacrylate glue used to mount the crystal to a glass slide for polishing was removed by soaking in acetone and subsequently rinsing in methanol. Fourier transform infrared (FTIR) spectra were obtained in transmission mode using a KBr window on a Bruker Tensor 37 FTIR spectrometer. The instrument uses a globar source, KBr beamsplitter, and Hyperion microscope with MCT detector. Spectra were obtained with 512 scans at a resolution of 2 cm^{-1}.

Spectra on a crystal ~30 μm thick showed nearly no mid-IR (MIR) light transmission. A second crystal was polished to 8-10 μm thickness and although still very dark in color, allowed for some MIR transparency. An FTIR spectrum of the 8-10 μm thick crystal is shown in Figure 3, baseline corrected to the region at 2500-4000 cm^{-1}. Although the spectra are dominated by interference fringes, neither C-H contamination from the glue nor detectible O-H in the structure of Fe-rich jeffbenite grown under hydrous conditions is observed.

Synchrotron Mössbauer spectroscopy

To evaluate the oxidation states of Fe in the synthetic jeffbenite, time-domain synchrotron-Mössbauer spectroscopy was conducted at Sector 3-ID-B of the Advanced Photon Source (APS), Argonne National Laboratory. A combination of a Si (111) double crystal monochromator and a 4-bounce inline high resolution monochromator was used to reduce the light energy bandpass to 1 meV at 14.4125 keV, which was then focused into a beam 15 μm in diameter using a Kirkpatrick-Baez type mirror. The APS storage ring was filled with 24 equally spaced radiation bunches giving pulses of 153 ns apart. The nuclear delay signal was recorded in the 21 – 128 ns time window of each pulse.

This is the peer-reviewed, final accepted version for American Mineralogist, published by the Mineralogical Society of America.
The published version is subject to change. Cite as Authors (Year) Title. American Mineralogist, in press.
DOI: https://doi.org/10.2138/am-2021-7852. http://www.minsocam.org/

Details of performing time-domain synchrotron-Mössbauer spectroscopy to extract hyperfine field parameters can be found in Alp et al. (1995). The synchrotron-Mössbauer spectra were collected with the same crystal that was used for X-ray diffraction (sample B8). Data were collected twice, once with the sample only and once with both the sample and a stainless steel foil, with the foil acting as the reference to determine the isomer shift. Time decay spectra were fitted using version 2.2.0 of the CONUSS software (Sturhahn, 2000) to obtain the hyperfine parameters of iron and the ferric-to-ferrous ratio in the sample.

The first attempt to fit the spectra used a two-doublet model after McCammon et al. (1997), where one doublet is assigned to Fe^{2+} and a second doublet is assigned to Fe^{3+}. For Fe^{2+}, the isomer shift is 1.285(6) mm/s and quadrupole splitting is 2.166(1) mm/s. For Fe^{3+}, the isomer shift is 0.301(3) mm/s and quadrupole splitting is 0.6077(5) mm/s.

The spectra were also fitted with a three-doublet model by adding an additional Fe^{2+} site. This three-doublet model assumes two Fe^{2+} sites and one Fe^{3+} site, which were distinguished by their hyperfine parameters. Although the improvement in the fit using the three-doublet model in place of the two-doublet model is not statistically significant, it is more consistent with site occupancy data from the single-crystal X-ray diffraction data as discussed below. The best fit curve to the sample-only spectrum is shown in Figure 4A. The corresponding energy domain spectrum is shown in Figure 4B. The isomer shift was fixed at 1.285 mm/s for both Fe^{2+} sites, while the quadrupole splitting and relative weight fraction were fitted and are 2.558(4) and 1.694(5) mm/s, respectively, for the quadrupole splitting. For the Fe^{3+} site, the fitted isomer shift is 0.578(3) mm/s and quadrupole splitting is 0.581(5) mm/s. These values are also given in Table 4 along with the values from the two-doublet model, and the values from McCammon et al. (1997) for their two TAPP diamond inclusions.

This is the peer-reviewed, final accepted version for American Mineralogist, published by the Mineralogical Society of America.
The published version is subject to change. Cite as Authors (Year) Title. American Mineralogist, in press.
DOI: https://doi.org/10.2138/am-2021-7852. http://www.minsocam.org/

RESULTS and DISCUSSION

Crystal Structure

Although the composition of jeffbenite appears to nearly overlap with that of a garnet, and the Raman spectrum of jeffbenite is very similar to garnet (Nestola et al. 2016), as noted by Finger and Conrad (2000), the crystal structure does not resemble garnet or the tetragonal garnet, majorite. In garnet the tetrahedra and octahedra do not share edges, whereas in jeffbenite the T2 tetrahedron shares an edge with the M2 octahedron. The density of jeffbenite synthesized here with approximate composition $(Mg_{0.60}Fe_{0.40})_4(Mg_{0.36}Fe_{0.64})_8(Mg_{0.65}Fe_{0.35})_8\,(Si)_4(Si_{0.94}Fe_{0.06})_8O_{48}$ from the microprobe data is calculated to be 3.93 g/cm^3, and that of a garnet with similar composition, $(Mg_{0.87}Fe_{0.13})_3Fe_2Si_3O_{12}$, is estimated to be 3.95 g/cm^3 based on an estimated cell edge of 11.468Å, cell volume of 1508.3 Å^3 and formula weight of 473.15 g. These are essentially indistinguishable, so that there is no clear density relationship between jeffbenite and garnet. The main difference is in the ratio of trivalent to divalent and tetravalent cations. The Fe-rich jeffbenite has slightly fewer than 3.0 Si per 12 oxygens and more than 2.0 trivalent cations per 12 oxygens as do most natural jeffbenite samples.

In the crystal structure of jeffbenite (Figure 1), there are three distinct oxygen sites, two tetrahedral sites (T1, T2), and three other cation sites where M1 is in eight-coordination with oxygen, and sites M2 and M3 are octahedral. All oxygen atoms are in 16*e* general positions, for a total of 48 oxygens per cell. O1 and O2 are each bonded to one T2, and one each of M1, M2, and M3. O3 is bonded to T1, M2 and M3. Site-specific electrostatic potentials are typical for oxygen sites in orthosilicate minerals (Smyth 1988) and are calculated to be 27.5V, 27.0V and 26.2V for

O1, O2, and O3 respectively, which are typical for non-hydroxyl oxygen positions in orthosilicate minerals.

The unit cell of jeffbenite appears to bear a strong relationship to that of zircon with body-centered tetragonal symmetry, a similar *a*-axis, and a tripled *c*-axis. In zircon, the two cation sites have $\overline{4}2m$ symmetry (Smyth and Bish, 1988), whereas in this structure the analogous T1 and M1 sites have just $\overline{4}$ symmetry. As noted by Harte et al. (1999), Bulanova et al. (2010), and Nestola et al (2016), Zr and Hf are significant trace elements in natural jeffbenite. Because of the close structural similarity to zircon, it might be possible for (0 0 1) lamellae of zircon structure enriched in Zr, Hf, U, and Th) to develop in natural jeffbenite, perhaps at inversion twin boundaries.

The T1 site is in a Wyckoff 4*b* position (4 per cell) with $\overline{4}$ symmetry, so all T – O distances are equivalent. The site is slightly compressed so that not all oxygen-oxygen tetrahedral edges are the same, with two long (2.81Å) and four short (2.58Å). The site appears to be fully occupied by Si with no indication of partial occupancy by heavier cations or significant cation vacancies. It is slightly smaller than T2 and shares no edges with other coordination polyhedra. Its electrostatic site potential of -49.4v is slightly deep but not atypical for tetrahedral Si sites.

The T2 site is in a Wyckoff 8*d* position (8 per cell) on a two-fold axis, so there are two long (1.67 Å) and two short (1.63 Å) T – O distances. The T2 is also significantly larger than T1 (Table 2) and shares an edge with an M2 octahedron. Occupancy refinement indicates the presence of a significant amount (6.0 ± 0.2 percent) of a heavier cation (ferric iron) at the site, although this is probably too little to see as a separate doublet in the Mössbauer spectrum. Finger and Conrad (2000) inferred 5 percent occupancy of Al in T2. In the final stages of the

refinement, the largest peak in the difference map was adjacent to T2 which might indicate that the heavy cation was occupying a slightly different position than the Si. In the final refinement the *x/a* position parameter of this partial atom was allowed to vary independent of that of the Si position (with the nearly isotropic displacement parameters of the two sites constrained to be equal) which resulted in a significant improvement of the R factor. The *x/a* parameters of the two sites are 0.1532(4) for Si and 0.222(3) for the Fe, whereas the *y/b* and *z/c* parameters are constrained by symmetry. The details of this position can be found in the CIF file.

The relatively large volume of the T2 tetrahedron (Table 3) may allow trivalent cation substitution which could lead to jeffbenite being compositionally distinct from garnet. The observation of ferric iron at this site is statistically robust due to the large difference in atomic number between Fe and Si and is consistent with Al substitution at this site reported by Finger and Conrad (2000). Anzolini et al., (2016) report that Ti substitution may increase the pressure stability range of jeffbenite, and chemical analyses of Ti-rich jeffbenites indicate partial substitution of Si by Ti. The T2 tetrahedral site would likely be the preferred site for Ti substitution.

The M1 cation site is in a 4*a* position at the origin and has $\overline{4}$ symmetry. The coordination may be seen as a tetrahedron, with four near oxygens at 2.14Å, but there are also four other oxygens at 2.58 Å (Table 3). The position is analogous to the Zr position in zircon, but with lower point symmetry. Distributing the total scattering to Mg and Fe cations, the occupancy refines to 60% Mg and 40% Fe. Because of the relatively large distances for even the close four anions (2.14 Å), much of the iron is likely ferrous, however the hyperfine parameters for Fe^{3+} also suggest that ferric iron likely occupies a highly distorted site, such as M1. The M1 site

might also accommodate larger-radius cations such as rare earths or Zr and Hf. The site potential of the site is calculated to be -22.4V, consistent with primarily divalent cation occupancy.

M2 is in an 8*d* position with site symmetry 2 and is a small, but fairly regular, octahedron. With occupancy split between Fe and Mg and assuming full occupancy, the refined occupancy is 64% Fe and 36% Mg. Polyhedral volume is 10.8 $Å^3$ (Table 3), compared to 10.8 $Å^3$ for Fe^{3+} in hematite and 13.4 $Å^3$ for Fe^{2+} in wüstite (Smyth and Bish, 1988), so most of this Fe is probably ferric. Indeed, this position is predominantly Al in natural jeffbenite (Finger and Conrad, 2000; Nestola et al 2016). However, it should be noted that the hyperfine parameters for Fe^{3+}, discussed below, are more consistent with tetrahedral and distorted octahedral coordination. The electrostatic potential calculated for this site is -34.3V (Table 3), consistent with primarily trivalent cation occupancy.

M3 is in an 8*c* position also with site symmetry 2. Occupancy modelled with Mg and Fe scattering factors and assuming no vacancy gives 65%Mg and 35% Fe. Polyhedral volume is 11.7$Å^3$, so it is slightly larger than M2 and much of the Fe is probably ferric. The electrostatic potential calculated for this site is -26.6V (Table 3), consistent with divalent and trivalent cation occupancy. In summary, the crystal structure study shows a diversity of cations site sizes and geometries with significant ferric iron in the larger T2 tetrahedral site giving fewer than 3.0 Si per twelve oxygen atoms.

Raman Spectroscopy

A detail of the Raman spectrum of synthetic ferromagnesian jeffbenite from this study is shown with deconvolution of the main bands in Figure 5A, along with a comparison to the natural jeffbenite Raman spectrum in Figure 5B. Based on work from Kolesov and Geiger,

(1998) on pyrope, Nestola et al. (2016) divided the Raman spectrum of jeffbenite into three regions. The 850-1060 cm^{-1} region was assigned to Si-O stretching modes, 490-640 cm^{-1} region to SiO_4 bending modes, and 300-400 cm^{-1} region to SiO_4 rotational modes. The peaks below 300 cm^{-1} were suggested to be either SiO_4 translational modes or Mg-O vibrations. Our spectra showed a similar pattern. The peaks described by Nestola et al. (2016) were also present in our spectra, except for some peaks in the low wavenumber region (at 284 cm^{-1}). However, most of our peaks were shifted to lower Raman frequencies, especially the peaks assigned to SiO_4 stretching and bending modes. These shifts are most likely caused by iron substitution in M1-M3 and T2 sites.

Raman spectra of garnet solid solutions have shown that their SiO_4 bending, rotational and stretching mode frequencies are affected by nearby cations (Kolesov and Geiger, 1998). Assuming that jeffbenite behaves similarly, and that our sample is enriched in iron compared to the aluminum in the sample of Nestola et al. (2016), this would explain the blue shift of the SiO_4 bending, rotational and stretching mode frequencies. Our spectra also showed several bands above 1000 cm^{-1}, but based on current information, it is hard to specify their nature. These could be overtone bands.

Synchrotron Mössbauer spectroscopy

In Table 5, the two-doublet model isomer shift and quadrupole splitting for Fe^{2+} and Fe^{3+} in synthetic ferromagnesian jeffbenite are compared to those reported by McCammon et al. (1997) for their two jeffbenite (TAPP) diamond inclusions. Whereas our quadrupole splitting, for both Fe^{3+} and Fe^{2+}, agree within uncertainty with those in McCammon et al. (1997) for TAPP, the isomer shift for both Fe^{3+} and Fe^{2+} in our sample are slightly larger. The slightly larger isomer shift likely indicates that both Fe^{3+} and Fe^{2+} in our sample have a larger mean metal-oxygen

distance (Burns 1994). This is consistent with the XRD structure refinement deduction of a larger metal-oxygen distance in our sample compared with the samples in McCammon et al. (1997).

The Fe^{2+} hyperfine parameters indicate octahedral coordination, and thus likely enrichment in M3 sites as suggested by McCammon et al. (1997). However, unlike the McCammon et al. (1997) sample, the M2 and M3 sites are similar in size in our sample, although M2 is slightly smaller. The relatively smaller M2 site in the McCammon et al. (1997) sample might be due to a high occupancy of Al^{3+} in the M2 site of natural jeffbenite, whereas our sample is Al-free and comprised 60% iron. Thus, it is possible that Fe^{2+} is also present in the M2 sites of our sample. The hyperfine parameter may suggest that significant occupation of the M1 site by Fe^{2+} is less likely.

Since the upper limit for the isomer shift of tetrahedral Fe^{3+} is 0.25 mm/s, while the lower limit for the isomer shift of octahedral Fe^{3+} is 0.29 mm/s (Burns 1994), our value of 0.301(3) suggests that most of the ferric iron in our sample has octahedral coordination (Figure 6). This is consistent with our XRD structure refinement that gave a site occupancy of 100% Si at the T1 site and only ~6% Fe (Fe^{3+}) at the T2 site. The similar quadrupole splitting parameters indicate that Fe^{3+} in our sample is likely mostly at a tetrahedral or distorted octahedral site (McCammon et al. 1997). It is likely that M1 contains most of the Fe^{3+} because the hyperfine parameters of Fe^{2+} showed that Fe^{2+} is unlikely to be at M1. Fe^{3+} can occupy the tetrahedral site, but this is only to be a small extent that is unlikely to change the $Fe^{3+}/\Sigma Fe$ value. Thus the large $Fe^{3+}/\Sigma Fe$ value indicates some Fe^{3+}could be at the M2 site, that is, if Fe^{2+} occupies most of both M2 and M3 sites, the $Fe^{3+}/\Sigma Fe$ value would be much smaller than the value determined from the Mössbauer spectra. Since the Mössbauer spectra show that $Fe^{3+}/\Sigma Fe = 0.65(1)$, and the ratio of

iron occupancy of the three M sites is 1:3.2:1.1, the ratio of Fe^{3+} to Fe^{2+} at the M2 site is likely to be 2:1. This assignment, although not definitive, is in agreement with general trends in the hyperfine parameters and assignments based on natural Al-rich jeffbenite (McCammon et al., 1997; Harris et al., 1997; Finger and Conrad, 2000). In summary, a two-doublet model fitting of the Mössbauer spectra gave the result that Fe^{3+} occupies the M1 and M2 sites, and Fe^{2+} occupies the M2 and M3 sites. Although the two-doublet model is in general in agreement with the previous study, this assignment needs to be reconciled with the relatively large distance between the M1 site and the closer four anions (2.14 Å), where one might expect a preference for Fe^{2+}.

In the three-doublet model, the quadrupole splitting of the Fe^{3+} site remains the same as the two-doublet model but the isomer shift shifts to a higher number, which would indicate a distorted geometry of the site with octahedral coordination (Dyar et al. 2006). M1 has the lowest effective coordination number and longest M-O distances of all the M sites and it is thus unlikely to be occupied by Fe^{3+}. Since between M2 and M3, M2 is slightly more distorted than M3, and as the amount of Fe in M2 sites is nearly equal to the amount of Fe^{3+} sites from the model fitting to the Mössbauer spectra, we assign Fe^{3+} to M2. That the two Fe^{2+} sites have the same isomer shift but distinct quadrupole splitting would be due to that quadrupole splitting is sensitive to site geometry (Dyar et al. 2006). We assign the Fe^{2+} site with the larger quadrupole splitting to the M1 site because the M1 polyhedron is more distorted than the M3 octahedron. Then the Fe^{2+} site with the smaller quadrupole splitting is assigned to the M3 site. The relative weight fraction of the M1, M2, and M3 sites obtained from the three-doublet model is 0.12:0.31:0.1, which is a ratio that is quite close to the one determined by XRD structure refinement that would then support the use of the three-doublet model to fit the Mössbauer spectra. In summary, a three-

doublet model fitting of the Mössbauer spectra gave the result that Fe^{3+} occupies the M2 site, and Fe^{2+} occupies the M3 and M1 sites.

IMPLICATIONS

Diamonds of superdeep origins in the transition zone or lower mantle, and especially the mineral inclusions contained within them, are important recorders of deep-mantle geochemistry and crustal recycling (e.g. Walter et al. 2011; Smith et al. 2018; Thomson et al. 2016). Jeffbenite is among those minerals known as inclusions in diamond that could be interpreted as representing components of subducted basaltic crust, with natural samples having been investigated showing bulk compositions similar to almandine (Nestola et al. 2016; McCammon et al. 1997; Harris et al. 1997; Zedgenizov et al. 2020) and with relatively high Fe^{3+} contents at 65-75% of the total iron (McCammon et a. 1997). Here, we explore solid solutions in jeffbenite in the Al-free, forsterite-fayalite-magnetite field with water present. A newly observed ferromagnesian jeffbenite phase was obtained, with implications for mantle mineralogy and diamond inclusion studies.

The sample was synthesized at 15 GPa and 1200 ºC and coexists with primitive clinopyroxene. This pyroxene is not unexpected as it has been observed to coexist with wadsleyite at pressures to about 18 GPa (Zhang and Smyth, 2020). It is therefore unlikely that the jeffbenite phase can only occur as a metastable retrograde inversion from a higher pressure phase such as bridgmanite. It appears that this phase has a true stability field within the Earth's transition zone at depths near 450 km under oxidizing and Fe-rich conditions despite its very close compositional overlap with garnet.

Jeffbenite, then, is not a garnet, but is similar to garnet in both density and composition. It is also similar to garnet in that even when grown under hydrous conditions at mantle P-T conditions the incorporation of water is only trace amounts, i.e. typically <200 ppm in kimberlite settings (e.g. Bell and Rossman 1992). The jeffbenite structure, however, is more closely related to zircon than to garnet. It is likely that jeffbenite is a stable phase in the transition zone at depths of 400 to 500 km in mafic compositions rich in ferric iron and/or aluminum. Because the synthesis was achieved directly at 15 GPa, it appears unlikely that jeffbenite is only a retrograde product of bridgmanite as has been suggested (Armstrong and Walter, 2012; Hayman et al., 2005; Zedgenisov et al., 2020).

The principal differences between jeffbenite and garnet appear to be both structural and compositional, rather than pressure-driven polymorphism. Published chemical analyses of jeffbenite (Harris et al., 1997; Harte et al, 1999; Kaminsky et al., 2001; McCammon et al., 1997; Armstrong and Walter, 2012; Nestola et al., 2016) uniformly show fewer than 3.0 Si and fewer than 3.0 divalent cations per 12 oxygen atoms. Finger and Conrad (2000) indicate about 5 percent Al substitution in T2 and we here document 6.0 percent ferric iron in T2. Aluminum or other trivalent cations have not been documented to substitute in the tetrahedral site in garnet at mantle pressures, although this substitution can occur at low pressure and high temperature. The greater diversity of cation site geometries and potentials in jeffbenite relative to garnet, then, allows the structure to accept ferric iron and Al into the larger tetrahedral site, T2. The polyhedral volume of T2 is larger than T1 largely because it shares an edge with M2. It appears, then, that the compositional range of jeffbenite does not overlap that of garnet, so jeffbenite may be a stable phase in regions of the transition zone rich in aluminum and/or ferric iron. This study has shown that Fe-rich jeffbenite is readily synthesized at transition zone PT conditions, but

400 leaves many questions to be addressed by further studies. We have begun to measure elasticity of
401 the current material, but have been unable to conduct further synthesis experiments to explore
402 the composition space due to current travel restrictions.
403

404 ## ACKNOWLEDGMENTS

405 Synthesis was supported by Bayerisches Geoinstitut at University of Bayreuth, Germany
406 and by US National Science Foundation grant EAR1416979 to JRS. This study was also
407 supported in part by the US National Science Foundation award EAR-1853521 to SDJ. This
408 research used resources of the Advanced Photon Source, a U.S. Department of Energy (DOE)
409 Office of Science User Facility operated for the DOE Office of Science by Argonne National
410 Laboratory under Contract No. DE-AC02-06CH11357. We also thank Neal Blair for access to
411 the FTIR microscope at Northwestern University. The authors thank the Associate Editor, two
412 anonymous referees, and the Technical Editor for constructive comments and suggestions.
413

REFERENCES CITED

Alp, E. E., Sturhahn, W., and Toellner, T. (1995) Synchrotron Mossbauer spectroscopy of powder samples. Nuclear Instruments and Methods in Physics Research Section B: Beam Interactions with Materials and Atoms, 97(1-4), 526-529.

Anzolini, C., Drewitt, J., Lord, O.T., Walter, M.J., and Nestola, F. (2016) New stability field of jeffbenite (ex-TAPP): Possibility of super-deep origin. American Geophysical Union Fall Meeting 2016, Abstract MR33A-2675.

Armstrong, L.S., and Walter, M.J. (2012) Tetragonal almandine pyrope phase (TAPP): retrograde Mg-perovskite from subducted oceanic crust? European Journal of Mineralogy, 24, 587-597.

Azavant, P., and Lichanot, A. (1993) X-ray scattering factors of oxygen and sulfur ions: An *Ab Initio* Hartree-Fock calculation. Acta Crystallographica, A49, 91-97.

Bell, D.R., and Rossman, G.R. (1992) The distribution of hydroxyl in garnets from the subcontinental mantle of southern Africa. Contributions, to Mineralogy and Petrology, 111, 161-178.

Bolfan-Casanova, N., Muñoz, M., McCammon, C., Deloule, E., Férot, A., Demouchy, S., France, L., Andrault, D., and Pascarelli, S. (2012) Ferric iron and water incorporation in wadsleyite under hydrous and oxidizing conditions: A XANES, Mössbauer, and SIMS study. American Mineralogist, 97, 1483-1493.

Bulanova, G.P., Walter, M.J., Smith, C.B., Kohn, S.C., Armstrong, L.S., Blundy, J., and Gobbo, L. (2010) Mineral inclusions in sublithospheric diamonds from Collier 4 kimberlite pipe, Juina, Brazil: subducted protoliths, carbonated melts and primary kimberlite magmatism. Contributions, to Mineralogy and Petrology, 160, 489-510.

437 Burns, R.G. (1994). Mineral Mössbauer spectroscopy: correlations between chemical shift and
438 quadrupole splitting parameters. Hyperfine Interactions, 91(1), 739-745
439 Cromer, D.T., and Mann, J. (1968) X-ray scattering factors computed from numerical Hartree-
440 Fock wave functions. Acta Crystallographica, A24, 321-325.
441 Dyar, M.D., Agresti, D.G., Schaefer, M.W., Grant, C.A., and Sklute, E.C. (2006) Mössbauer
442 spectroscopy of Earth and planetary materials. Annual Reviews of Earth and Planetary
443 Sciences, 34, 83-125.
444 Finger, L.W., and Conrad, P.G. (2000) The crystal structure of "tetragonal almandine-pyrope
445 phase" (TAPP): A reexamination. American Mineralogist, 85, 1804-1807.
446 Harris, J., Hutchison, M.T., Hursthouse, M. Light, M., and Harte, B. (1997) A new tetragonal
447 silicate mineral occurring as inclusions in lower-mantle diamonds. Nature, 387, 486-488.
448 Harte, B., Harris, J.W., Hutchison, M.T., Watt, G.R., and Wilding, M.C. (1999): Lower mantle
449 mineral associations in diamonds from Sao Luiz, Brazil. in ''*Mantle petrology: field*
450 *observations and high pressure experimentation: a tribute to Francis R. (Joe) Boyd*'', Fei, Y.
451 Bertka, C.M., Mysen, B.O., eds., The Geochemical Society, Houston, TX, 125–153.
452 Hayman, P.C., Kopylova, M.G., and Kaminsky, F.V. (2005) Lower mantle diamonds from Rio
453 Soriso (Juina area, Mato Grosso, Brazil). Contribution to Mineralogy and Petrology, 149,
454 430-445.
455 Kaminsky, F.V., Zakharchenko, O.D., Davies, R., Griffin, W.L., Khachatryan, G.K., and
456 Shiryaev, A.A. (2001): Superdeep diamonds from the Juina area, Mato Grosso State, Brazil.
457 Contributions to Mineralogy and Petrology, 140, 734–753.
458 Kolesov, B.A., and Geiger, C.A (1998) Raman spectra of silicate garnets. Physics and Chemistry
459 of Minerals, 25, 142-151.

McCammon, C.A., Stachel, T., and Harris, J.W. (1997) Ferric iron contents of mineral inclusions in diamonds from São Luis: a view into the lower mantle. Science, 278, 434-436.

Momma, K., and Izumi, F. (2011) VESTA 3 for three-dimensional visualization of crystal, volumetric and morphology data. Journal of Applied Crystallography, 44, 1272-1276.

Nestola, F., Burnham, A.D., Peruzzo, L., Tauro, L., Alvaro, M. Walter, M.J., Gunter, M., Anzolini, C., and Kohn, S.C. (2016) Tetragonal almandine-pyrope phase, TAPP, finally a name for it, the new mineral jeffbenite. Mineralogical Magazine, 80, 1219-1232.

Smith, E.M., Shirey, S.B., Richardson, S.H., Nestola, F., Bullock, E.S., Wang, J., and Wang, W. (2018) Blue boron-bearing diamonds from the Earth's lower mantle. Nature, 560, 84-87.

Smyth, J.R., and Bish, D.L. (1987) Crystal Structures and Cation Sites of the Rock-Forming Minerals. Boston: Allen & Unwin, London, 358pp.

Smyth, J.R. (1988) Electrostatic characterization of oxygen sites in minerals. Geochimica et Cosmochimica Acta, 53, 1101-1110.

Smyth, J.R., Bolfan-Casanova, N., Avignant, D., El-Ghozzi, M., and Hirner, S.M. (2014) Tetrahedral ferric iron in oxidized hydrous wadsleyite. American Mineralogist, 99, 458-466.

Sturhahn, W. (2000). CONUSS and PHOENIX: Evaluation of nuclear resonant scattering data. Hyperfine Interactions, 125(1-4), 149-172.

Thomson, A.R., Walter, M.J., Kohn, S.C., and Brooker, R.A. (2016) Slab melting as a barrier to deep carbon subduction. Nature, 529, 76-79.

Walter, M.J., Kohn, S.C., Araujo, D., Bulanova, G.P.,Smith, C.B., Gaillou, W., Wang, J., Steele, A., and Shirey, S.B. (2011) Deep mantle cycling of oceanic crust: evidence from diamonds and their mineral inclusions. Science, 334, 54-57.

Woodland, A.B., and Angel, R.J. (1998) Crystal structure of a new spinelloid with the wadsleyite structure in the system Fe_2SiO_4 – Fe_3O_4 and implications for the Earth's mantle. American Mineralogist, 83, 404 – 408.

Zedgenisov, D., Kagi, H., Ohtani, E., Tsujimori, T., and Komatsu, K. (2020) Retrograde phases of former bridgmanite inclusions in superdeep diamonds. Lithos, 370-371, 105659.

Zhang, L., and Smyth, J.R. (2020) Fe^{2+} substitution in coexisting wadsleyite and clinopyroxene under hydrous conditions: Implications for the 520-km discontinuity. Physics and Chemistry of Minerals, 47, 2.

This is the peer-reviewed, final accepted version for American Mineralogist, published by the Mineralogical Society of America.
The published version is subject to change. Cite as Authors (Year) Title. American Mineralogist, in press.
DOI: https://doi.org/10.2138/am-2021-7852. http://www.minsocam.org/

Table 1. Chemical composition from EPMA, taken from the average of fifteen points.

Oxide	Weight Percent**	Cations	per 12 Oxygens
SiO_2	34.39 (0.17)	Si	2.81
Al_2O_3	0.31 (0.02)	Al	0.03
MgO	18.63 (0.14)	Mg	2.25
FeO	44.23 (0.33)		
Total	97.57		
FeO*	15.48	Fe^{2+}*	1.05
Fe_2O_3*	32.07	Fe^{3+}*	2.05
Total*	100.88	Total	8.19

*Values recalculated from Mössbauer-determined $Fe^{3+}/\Sigma Fe$.

**1σ standard deviation given in parenthesis.

This is the peer-reviewed, final accepted version for American Mineralogist, published by the Mineralogical Society of America.
The published version is subject to change. Cite as Authors (Year) Title. American Mineralogist, in press.
DOI: https://doi.org/10.2138/am-2021-7852. http://www.minsocam.org/

Table 2. Crystal data and results of refinement for Fe-Mg jeffbenite.

Crystal Data	
Chemical Formula	$Mg_{2.62}Fe_{2.50}Si_{2.88}O_{12}$ Space Group
$I\bar{4}2d$ (#122)	
Unit Cell Dimensions	
a(Å)	6.6449(3)
c(Å)	18.4823(9)
V(Å^3)	816.08(9)
Z	4
X-ray density (g/cm^3)	3.93
μ (mm^{-1})	5.146
Data Collection	
Diffractometer	Bruker P4 (APEX II detector)
Radiation, wavelength (Å)	Mo$K\alpha$, 0.71073
Crystal	Opaque black irregular fragment
Crystal size	0.12 x 0.10 x 0.08 mm^3
Temperature (K)	293(2)
Number refl. Measured	12258
$R\sigma$	0.0306
Rint	0.0706
Number unique	1061
θmax	37.5º
Index range	h ± 11, k ± 11, l ± 31
Data completeness (%)	100
Parameter Refinement	
Reflections, restraints, parameters	1061, 0, 54
$R_1[I > 2\sigma(I)]$, R_1(all)	0.0278, 0.0403
GoF (F_2)	1.064
Flack *x (Parson's method)*	0.05(2)

This is the peer-reviewed, final accepted version for American Mineralogist, published by the Mineralogical Society of America.
The published version is subject to change. Cite as Authors (Year) Title. American Mineralogist, in press.
DOI: https://doi.org/10.2138/am-2021-7852. http://www.minsocam.org/

Table 3. Selected cation–oxygen bond distances, distortion parameters, and electrostatic potentials for Fe-Mg jeffbenite.

Perameter	Value	Bond	Distance (Å)
T1 – O3 (4x) (Å)	1.630(2)	M2 – O1 (2x)	2.123(3)
T1 Quad. El.	1.0152	M2 – O2 (2x)	2.000(3)
T1 – Ang.Var.	56.22	M2 – O3 (2x)	1.948(3)
T1 Poly. Vol. (Å^3)	2.174	Mean M2 – O	2.024
T1 Occupancy	100% Si	M2 Quad. El.	1.0127
Electrostatic Pot. (V)	-49.39	M2 Ang. Var.	39.00
		M2 Poly. Vol. (Å^3)	10.86
T2 – O1 (2x)	1.670(3)	M2 Occupancy	36%Mg 64%Fe
T2 – O2 (2x)	1.629(3)	Electrostatic Pot. (V)	-34.32
Mean T2 – O	1.650		
T2 Quad. El.	1.0249		
T2 Ang. Var.	105.25		
T2 Poly. Vol. (Å^3)	2.219		
T2 Occupancy	94%Si 6%Fe	M3 – O1 (2x)	2.054(3)
Electrostatic Pot. (V)	-46.85	M3 – O2 (2x)	2.148(3)
		M3 – O3 (2x)	2.039(3)
M1 – O1 (4x)	2.140(3)	Mean M3 – O	2.080
M1 – O2 (4x)	2.576(3)	M3 Quad. El.	1.0198
Average of 8	2.358	M3 Ang. Var.	64.70
M1 Poly. Vol. (Å^3)	21.42	M3 Poly. Vol. (Å^3)	11.66
M1 Occupancy	60%Mg 40%Fe	M3 Occupancy	65%Mg 35%Fe
Electrostatic Pot. (V)	-22.26	Electrostatic Pot. (V)	-26.72

This is the peer-reviewed, final accepted version for American Mineralogist, published by the Mineralogical Society of America.
The published version is subject to change. Cite as Authors (Year) Title. American Mineralogist, in press.
DOI: https://doi.org/10.2138/am-2021-7852. http://www.minsocam.org/

565 **Table 4.** Comparison of hyperfine Mössbauer parameters for ferromagnesian jeffbenite sample
566 BZ238A with $Fe^{3+}/\Sigma Fe = 0.74(8)$ and BZ243A with $Fe^{3+}/\Sigma Fe = 0.66(8)$ from McCammon et
567 al. (1997) compared with synthetic jeffbenite in this study with $Fe^{3+}/\Sigma Fe = 0.65(1)$ (two-
568 doublet model) or 0.58(1) (three-doublet model).
569

Sample	Isomer shift (mm/s)	Quadrupole splitting (mm/s)	Reference
Fe^{2+}			
BZ238A	1.03(19)	2.39(39)	McCammon et al. (1997)
BZ243A	1.10(3)	2.04(6)	McCammon et al. (1997)
B8	1.285	2.166(1)	This study (two doublet)
B8	1.285	2.558(4)	This study (three doublet)
B8	1.285	1.694(5)	This study (three doublet)
Fe^{3+}			
BZ238A	0.15(8)	0.57(15)	McCammon et al. (1997)
BZ243A	0.17(2)	0.69(3)	McCammon et al. (1997)
B8	0.301(3)	0.6077(5)	This study (two doublet)
B8	0.578(3)	0.581(2)	This study (three doublet)

570
571
572
573

This is the peer-reviewed, final accepted version for American Mineralogist, published by the Mineralogical Society of America.
The published version is subject to change. Cite as Authors (Year) Title. American Mineralogist, in press.
DOI: https://doi.org/10.2138/am-2021-7852. http://www.minsocam.org/

Figures

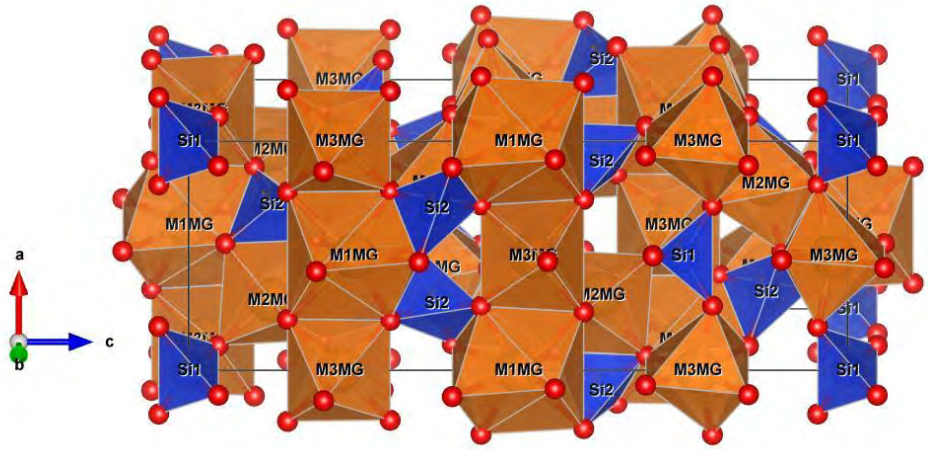

FIGURE 1. Crystal structure (inverse) of Fe-rich jeffbenite viewed along a direction close to the *b* axis (*c*-horizontal). Figure was drawn using VESTA, developed by Momma and Izumi (2011).

This is the peer-reviewed, final accepted version for American Mineralogist, published by the Mineralogical Society of America.
The published version is subject to change. Cite as Authors (Year) Title. American Mineralogist, in press.
DOI: https://doi.org/10.2138/am-2021-7852. http://www.minsocam.org/

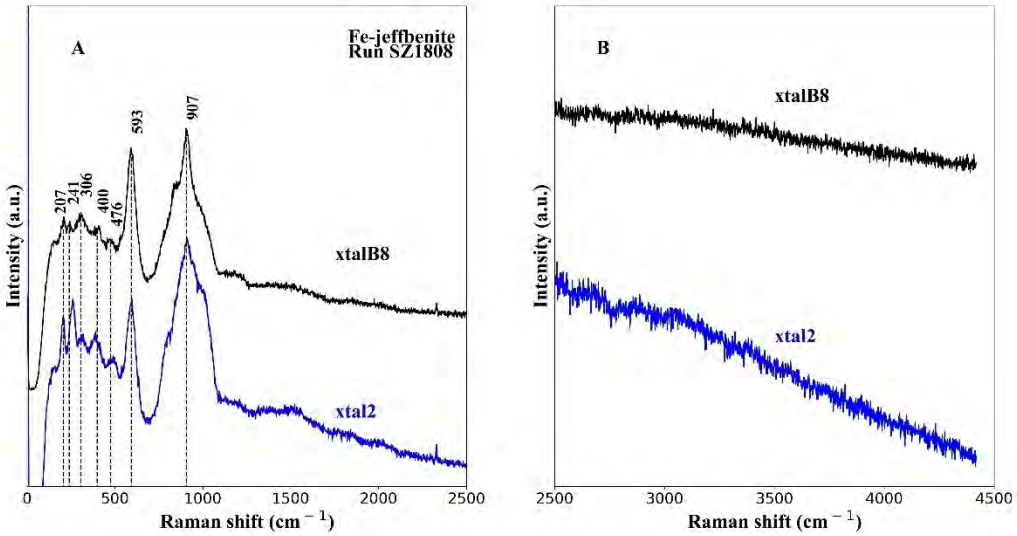

581

582 **Figure 2.** Raman spectra of synthetic ferromagnesian jeffbenite from (A) 0-2500 cm^{-1} and in (B)
583 from 2500-4500 cm^{-1} on an expanded vertical scale, showing the absence of detectible O-
584 H Raman modes. The spectrum in black was taken on the same crystal used in the X-ray
585 diffraction study (sample xtalB8) and in blue, another crystal (xtal2) chosen at random.
586 All spectra are shown as-measured, without baseline corrections. The small, sharp peak at
587 2330 cm^{-1} is from the vibrational mode of N_2 in air.

588

This is the peer-reviewed, final accepted version for American Mineralogist, published by the Mineralogical Society of America.
The published version is subject to change. Cite as Authors (Year) Title. American Mineralogist, in press.
DOI: https://doi.org/10.2138/am-2021-7852. http://www.minsocam.org/

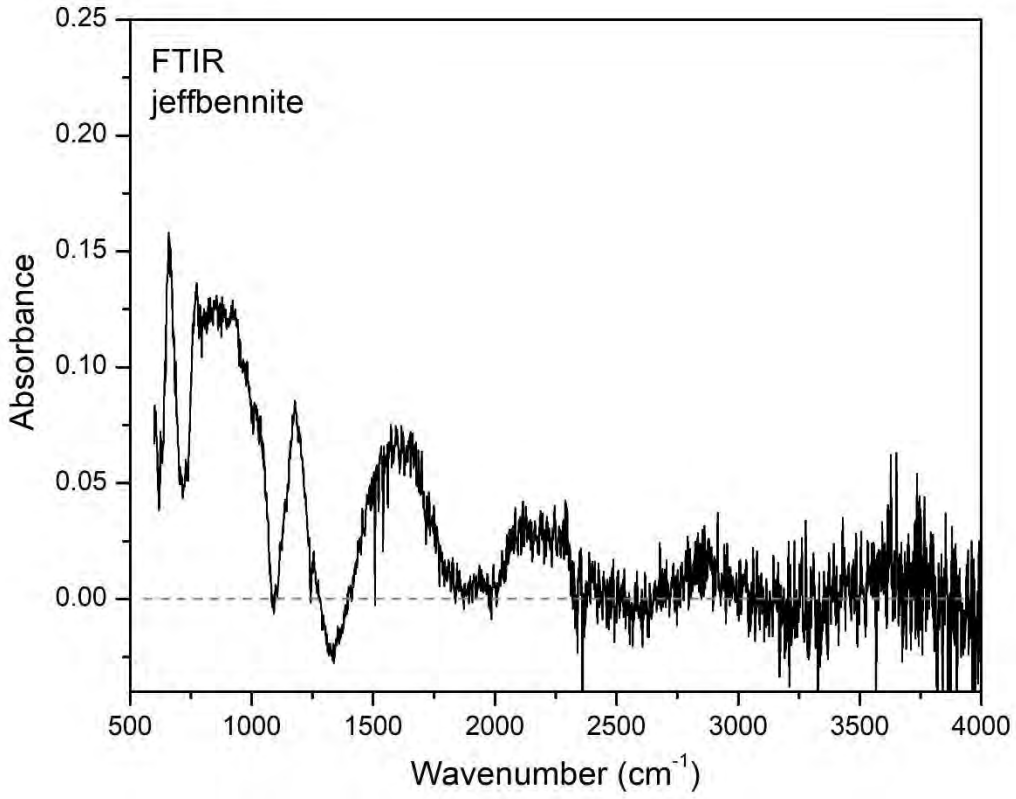

589

590

591 **FIGURE 3.** Unpolarized and baseline corrected FTIR spectra of Fe-rich jeffbennite crystal

592 double-side polished to 8-10 μm thickness. The spectrum is dominated by interference

593 fringes, but is free of contamination from the glue used to polish the crystal as would

594 have been evident by strong C-H absorbance at ~2900 cm^{-1}. There is no indication of OH

595 in the Fe-rich jeffbenite grown under hydrous conditions.

596

597

598

This is the peer-reviewed, final accepted version for American Mineralogist, published by the Mineralogical Society of America.
The published version is subject to change. Cite as Authors (Year) Title. American Mineralogist, in press.
DOI: https://doi.org/10.2138/am-2021-7852. http://www.minsocam.org/

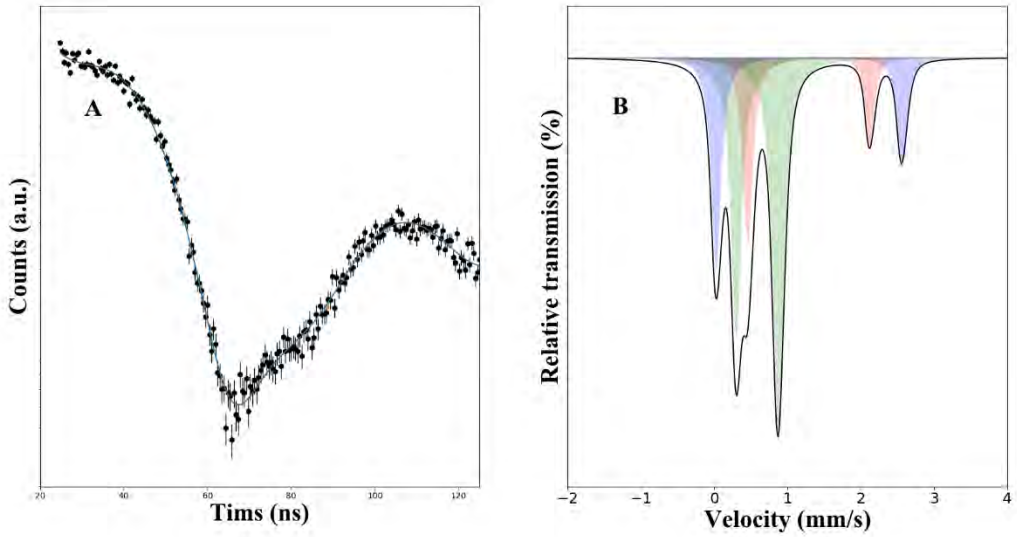

599

600 **FIGURE 4.** Time domain synchrotron-Mössbauer spectrum without stainless steel foil (A). The

601 fitted curve was obtained using CONUSS 2.2.0 and has $\chi^2 = 1.80$. Energy domain

602 spectrum of the best fit hyperfine model parameters (three-doublet model) (B). The blue

603 and red-shaded doublets correspond to two Fe^{2+} sites and the green-shaded doublet

604 corresponds to Fe^{3+}. Based on the fitted ratios we obtain a value of $Fe^{3+}/\Sigma Fe = 0.58(1)$.

605

This is the peer-reviewed, final accepted version for American Mineralogist, published by the Mineralogical Society of America.
The published version is subject to change. Cite as Authors (Year) Title. American Mineralogist, in press.
DOI: https://doi.org/10.2138/am-2021-7852. http://www.minsocam.org/

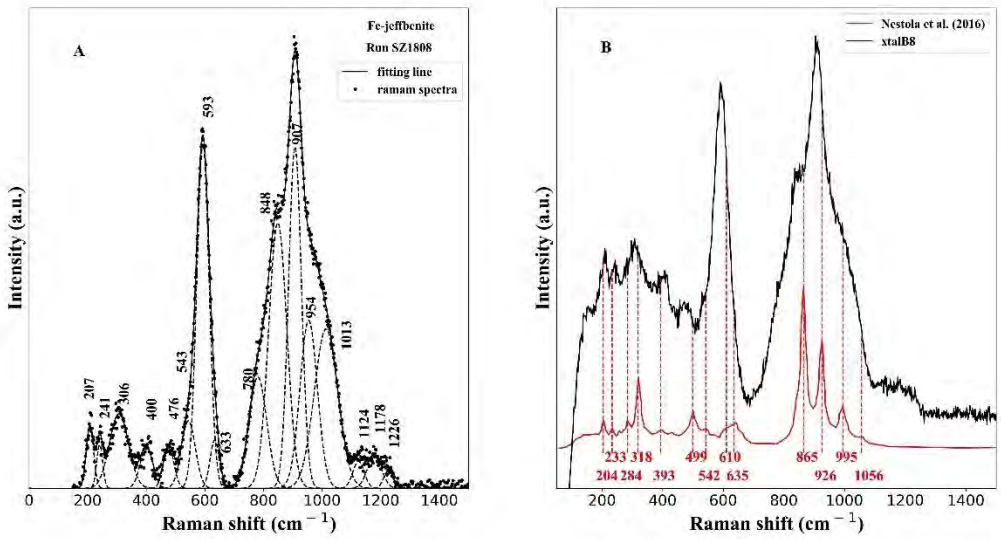

606

607 **FIGURE 5.** (A) Baseline corrected deconvolution of a Raman spectrum of Fe-rich jeffbenite,

608 sample B8 used in the X-ray diffraction study. (B) comparison of the raw (uncorrected)

609 Raman spectrum of Fe-rich jeffbenite with a natural jeffbenite found as a diamond

610 inclusion with approximate formula $(Mg_{2.62}Fe_{0.27})(Al_{1.86}Cr_{0.16})(Si_{2.82}Al_{0.18})O_{12}$ from

611 Nestola et al. (2016).

612

613

614

This is the peer-reviewed, final accepted version for American Mineralogist, published by the Mineralogical Society of America.
The published version is subject to change. Cite as Authors (Year) Title. American Mineralogist, in press.
DOI: https://doi.org/10.2138/am-2021-7852. http://www.minsocam.org/

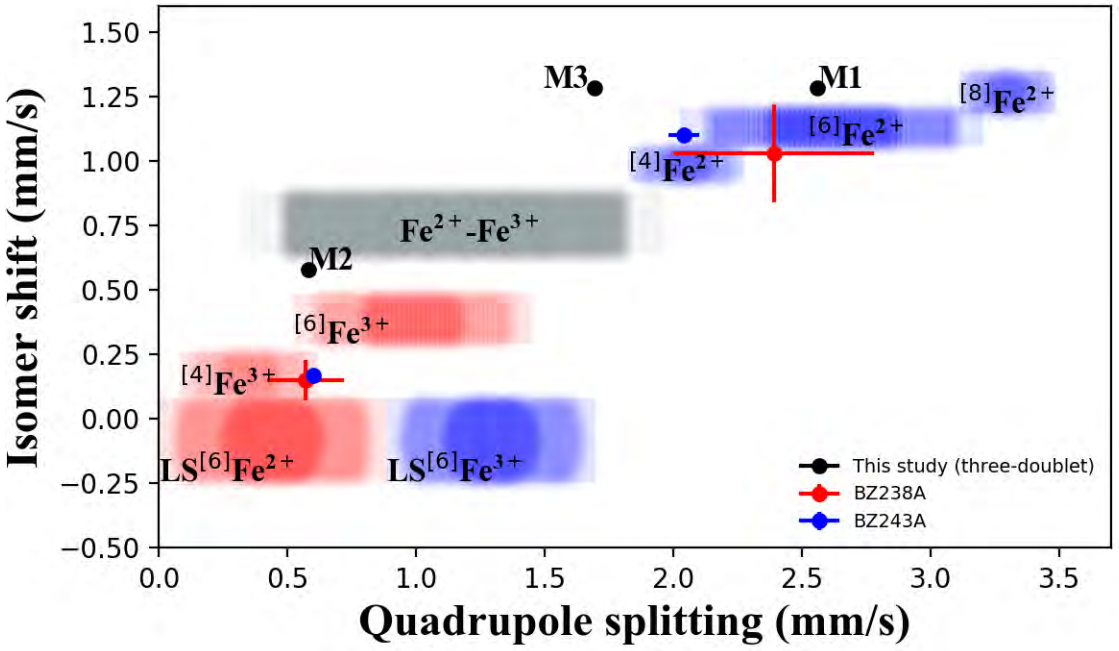

615

616 **FIGURE 6.** Mössbauer parameters of Fe assigned to M1, M2, and M3 sites in jeffbenite from
617 this study and the samples BZ238A and BZ243A from McCammon et al. (1997). Error
618 bars show uncertainty in the fits for each doublet. Shaded regions show the classification
619 of iron coordination and oxidation state from a large dataset of rock-forming minerals
620 (modified from Dyar et al. 2006). The superscript numbers in brackets indicate
621 coordination number, oxidation state is indicated by the ionic charge, and LS indicates
622 the low-spin state.

623